Molecular dynamics simulation of an activated transfer reaction in zeolites

Pierfranco Demontis, Giuseppe B. Suffritti, and Antonio Tilocca
Dipartimento di Chimica, Universita' degli studi di Sassari, Via Vienna 2, I-07100 Sassari, Italy

(Received 19 February 1999; accepted 1 July 1999)

The activated transfer of a light particle between two heavier species in the micropores of silicalite and ZK4 zeolites has been studied through molecular dynamics (MD) simulations. A three-body potential controls the exchange of the light particle between the heavier ones; an effective barrier of a few k_BT separates the two stable regions corresponding to symmetric ''reactant'' and ''product'' species. Harmonic forces always retain the reactants at favorable distances so that in principle only the energetic requirement must be fulfilled for the transfer to occur. The rate constant for the process (obtained from a correlation analysis of equilibrium MD trajectories) decreases by more than one order of magnitude when the barrier height is increased from $2k_BT$ to $5k_BT$ following an Arrhenius-type behavior. The transfer rates are always lower in ZK4. When the reaction is studied in a liquid solvent the calculated rate constants are closer to those obtained in silicalite. Since with this model the diffusive approach of the reactants is almost irrelevant on the reactive dynamics, only the different ability of each environment to transfer the appropriate energy amount to the reactants and then promote the barrier passage could be invoked to explain the observed behavior. We found that structural, rather than energetic, effects are mainly involved on this point. The lower efficiency of ZK4 seems to arise from the frequent trapping of the reactive complex in the narrow ZK4 windows in which the transfer is forbidden and from the weaker interaction of the reactive complex with the host framework compared to silicalite. © *1999 American Institute of Physics.* [S0021-9606(99)51736-4]

INTRODUCTION

Computer simulations[1] represent today a valuable tool in the study of many chemical processes involved in the catalytic action of zeolites. In shape-selective processes reactions are controlled by merely physical constraints which determine the (often different) diffusivities of reactant and/or products and their mixtures; molecular dynamics (MD) simulations have definitely proven to give good results in predicting and understanding such effects.[2] Nevertheless, shape selectivity is only one of the many aspects of the catalytic behavior of zeolites. There are some other points of considerable interest mainly connected to the direct effect of the topology and energetics of the framework on the reaction dynamics. Due to the complex features of reactive processes in zeolites a detailed knowledge of the microscopic steps involved in many catalytic reactions is still lacking.

As a first step to highlight some basic features of the zeolites activity we began to explore the energy exchanges between framework and sorbates:[3] MD simulations of the vibrational relaxation of diatomic molecules in silicalite showed that resonance effects are very important in the deactivation of excited molecules. In particular it was shown that these effects favor the relaxation of molecules whose oscillation frequency falls in the range of the normal vibrational modes of the framework. While this point may seem obvious on the basis of simple classical-mechanics rules, it is very important that these phenomena can be well reproduced with the simple zeolite model adopted. Indeed, the way and the rate at which energy is exchanged between the sorbate species and the environment represent a crucial point in the success of many condensed-phase reactions. Therefore a realistic reproduction of such effects should be the starting point of any meaningful study of reactive processes, while at the same time it is desirable to satisfy such requirement with a model as simple (that is little CPU-time demanding) as possible. The results of Ref. 3 proved that a harmonic model for the framework is fairly suitable in this respect; thus it can be adopted to develop further simulation studies of reactive processes. We then proceeded with the study of a dissociation-recombination reaction in silicalite.[4–6] Such kind of processes, exploiting many of the specific properties of zeolites, result particularly suitable as a starting point to obtain comparative information on the catalytic activity of different zeolitic hosts. Radical processes are usually not activated, thus a statistically meaningful number of *reactive* trajectories may be easily generated and examined by dissociating a stable molecule in different initial conditions and following its subsequent dynamics. There the main purpose was to get insight into the effectiveness of a zeolite in promoting the recombination of radicals after having controlled their dissociation and absorbed the excess energy. The comparison with the same process carried out in a dense liquid turned out to be very useful in the interpretation of the results and in understanding the correlation between the environment topology and the recombination path. These results showed how a simple, effective approach may in many cases lead to detailed, albeit nonspecific, information on the dynamics of a nonactivated reactive process in zeolites. Following this direction the next, obvious step is the study of an *activated* process. In this case an energetic barrier that lies between the stable states must be surmounted before a tran-

sition can occur. The additional energetic requirement can shift the reaction rates to rather low values, depending on the barrier height. For example, in the present work the time required for the activation along the reaction coordinate may in some cases be longer than 200 ps (for the highest barrier studied). Now the main purpose is to see how the surrounding environment can shift the required energy to the reactants and drive them along the reaction coordinate, finally allowing the barrier crossing. The triatomic transfer reaction, proposed and studied in a simple solvent by Allen and Schofield,[7,8] is very different from the radical encounter mentioned before mainly because both the breaking and the formation of bonds are now involved. In the previous study the energy needed to dissociate the molecule was provided from the outside (by simulating a photodissociation process) and we were only concerned in the eventual ''remaking'' of the broken chemical bond. Now the action of the environment is more complex, as the overall process is. Moreover, for activated processes, the transitions between stable species become *rare* events if the height of the reaction barrier is as large as several k_BT. Rare events are dynamical processes which occur so infrequently that it is impractical to obtain quantitative information about them through straightforward trajectory calculations; therefore special techniques are required to frequently simulate them.[9,10] In the present study we exploit the fact that the reactants are always kept close to the reaction distance through harmonic restoring forces so that they are forced to frequently collide and, if the energetic and steric requirements are met, finally react. These constraints, along with the low barriers adopted, allow obtaining kinetic data from standard, equilibrium MD simulations. Rate constants are directly obtained from the time correlation function of the fluctuations of a variable suitable to describe the reactant (or product) species (vide infra). As will be pointed out below, the application of this method is suitable as long as the barrier height is not too high ($\leqslant 5k_BT$). With higher barriers, even with the imposed constraints, the system would be trapped in a stable state for such a long time that the only practical choice to study the transition would be the standard ''reactive flux'' methods.[9] The constraints imposed on the reaction complex considerably limit the diffusive approach of the reactants and the eventual separation of the products. While this may seem a too serious restriction, it allows us to roughly ''isolate'' the activation step, which becomes the main aspect of the reaction dynamics, thus simplifying its study. In other words we mostly ignore the environment influence on the relative diffusion of the reactive species (arising by their confinement in the zeolitic host) in order to concentrate on the way in which a particular microporous structure can lead to the barrier passage.

The effect of the environment on this process can be illuminated by examining the variations in the reaction rate and dynamical behavior when changing the microporous structure surrounding the guest species. We examine here two common zeolite structures: silicalite[11] and ZK4.[12] They are characterized by internal cavities of different shapes and dimensions; therefore the sorbed species will experience much different reaction fields inside them. Important information about their influence on the reaction rates will be obtained by a detailed comparison of the structural and dynamical data arising from the MD simulations.

It should be remarked that within the adopted model we considered intermolecular van der Waals forces only: the solvent-solute interactions are weak and short-range. Previous theoretical studies[13] show that reactions of this kind (e.g. neutral atom exchange in rare gas solvents[14–16]) are usually characterized by smaller solvent effects compared to exchange reactions in which long-range, strong interactions (both of Coulombic and ion-dipole nature, like bimolecular substitutions of alkyl halides by anions in polar solvents[17–20]) are active. For example, the dynamics of energy flow into the reactants is much more complex for S_N2 reactions involving polar and charged species: a larger number of solvent atoms simultaneously take part in the energy transfer to the reactants compared with the $Cl+Cl_2$ model system.[16,19] A substantial reorganization of the solvent structure always precedes the reaction for the strongly interacting system while such effect is not observed for the weakly coupled case. Moreover the constraints imposed on the relative diffusion of the reactants could further level off the differences between the silicates and the liquid solvent. Greater differences between the zeolites and the liquid would probably result if the reactants were allowed to separate by releasing the harmonic constraints imposed. Due to caging effects (absent in the silicate pores) the bimolecular encounter in the liquid would be more hindered and less probable, but at the same time, whenever the reactants get trapped in the same solvent cage, the atom transfer should be favored: repeated collisions would occur until the steric and energetic requirements for the barrier crossing will be eventually met.[21]

It should be remarked that the two silicate structures considered are the *all-silica* analogues of synthetic zeolites ZSM-5 and A, which are of considerable interest for their widespread applications.[22] In particular their catalytic properties are due to the presence in the cavities of charge-compensating protons or metal cations that can act as Brönsted or Lewis acid sites. Depending on the zeolite crystal structure many catalytic reactions show very different paths and rates. These complex phenomena are related to the strong interactions between charged reactive intermediates and the intense, variable electric fields present in the micropores, as well as to the possible direct involvement of the protons bonded to the framework oxygens in the reaction mechanism. The simple transfer reaction occurring in the all-silica zeolites considered in this work is considerably easier to model and the perturbation that each framework structure induces on the reaction system is small. The success of the reaction depends only on the activation of the reactants driven by the topology of the zeolite through collisional energy exchanges. The different confinement of the reaction complex will be the *only* factor affecting reaction rates both through energetic and steric effects. Therefore we do not expect large differences in the reaction rates, as long as only the structure of the surrounding medium is changed while the forces exerted by the environment on the reactants are always kept weak and short-range. We chose to study such kind of reactions on analogous grounds to those that

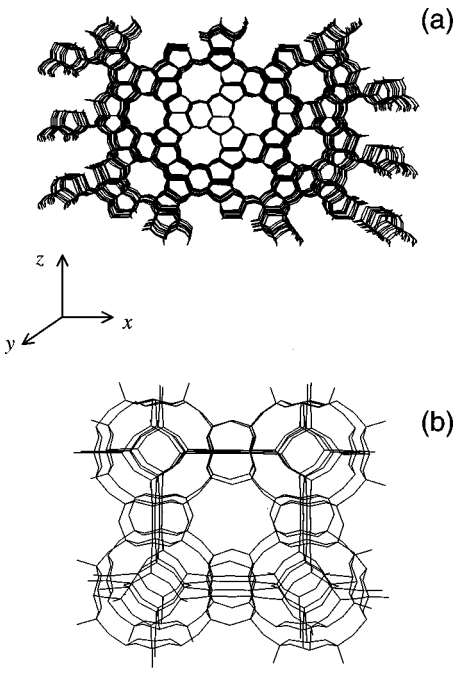

FIG. 1. (a) View of the pore structure of silicalite, pointing along the straight channels. (b) Structure of ZK4, showing the central α-cage.

stimulated many previous extensive studies of $X+X_2$ model reactions in rare gas solvents:[15,21,23] the relative simplicity of the interactions and of the model describing them allows to capture and understand in a great detail many general features of such processes, with particular emphasis on the solvent interaction with the reagents.[16] The dynamics of more complex reactions, besides being more difficult to simulate and understand, involves many further effects that may partially obscure the general features of the (crystalline) environment activity in which we are primarily interested. Clearly, aspects connected to charge transfer and solvation of the reaction system, as well as to the influence of the relative diffusion of the reactants are undoubtedly important and deserving of further studies, but in this paper we shall concentrate on the dynamics of a ''constrained'' transfer process entailing only short-range solvent–solute interactions. We believe that several interesting features of each zeolite structure highlighted with this model could be general enough to be, at least partially, extended to more complex reactive processes.

MODEL, METHOD AND CALCULATIONS

The structure of silicalite [Fig. 1(a)] is made of straight channels intersecting orthogonally with sinusoidal channels both with diameter of about 5.5 Å (the intersections diameter is about 9 Å); ZK4 microporous structure [Fig. 1(b)] is made of large spherical cages (diameter ~11.4 Å) connected by narrow windows about 4.2 Å wide. The MD runs were carried out in the microcanonical (*NVE*) statistical ensemble at about 300 K, both in silicalite and ZK4. The simulation boxes consisted of 2 unit cells (superimposed along *z*) for silicalite and 1 unit cell for ZK4, both corresponding to a total of 576 framework atoms. We verified that larger cells (up to 2304 atoms) give rise to negligible differences from the present results. Simulations with a liquid solvent, consisting of 256 LJ spheres modeling tetrachloromethane,[5] were carried out in the same conditions.

We are interested in the transfer of a light particle (labeled *C*) between two heavier, identical, ones:

$$A-C\cdots B\rightarrow A\cdots C-B. \tag{1}$$

The three particles remain always close to each other during the simulation; thus this process could also approximately represent a unimolecular rearrangement occurring within a tightly bound reaction complex *A-C-B*. The dynamics of the transfer has been followed according to a model proposed by Allen and Schofield[7] with some modifications. The *A* and *B* particles have the mass *M* of xenon and interact with each other and with the zeolitic oxygen atoms via a 12-6 Lennard-Jones (LJ) potential with xenon-like self-interaction parameters:[24] $\sigma=4.064$ Å, $\epsilon=1.87$ kJ mol^{-1} (the LJ parameters for the interaction with the oxygens were obtained from the combining rules[1] with $\sigma=2.529$ Å and $\epsilon=1.51$ kJ mol^{-1} for the oxygen atoms[25]). In all simulations the *m/M* ratio was fixed to 0.1 (*m* being the *C* particle mass). Compared to the original model an additional LJ interaction between the *C* species and the environment was introduced. It should be remarked that in this process the dominant interaction is between the ''solvent'' and the two larger bodies that significantly shield the *C* particle from directly interacting with the surrounding bath. Therefore the choice of the LJ parameters for the *C* species is not crucial; in any case the adopted values are only intended to model a significantly smaller species than xenon. For this purpose the parameters of fluorine[1] ($\sigma=2.83$ Å, $\epsilon=0.439$ kJ mol^{-1}) have been chosen.

The total internal potential of the reaction complex is then

$$V_{\rm int}=V_{\rm LJ}(\mathbf{r}_A,\mathbf{r}_B)+V_3(\mathbf{r}_A,\mathbf{r}_B,\mathbf{r}_C)+V_R(\mathbf{r}_A,\mathbf{r}_B). \tag{2}$$

The first term is the Lennard-Jones interaction between *A* and *B*. The second term is the three body potential which controls the motion of the particles within the reaction complex as proposed by Allen and Schofield:[7]

$$V_3(\mathbf{r}_A,\mathbf{r}_B,\mathbf{r}_C)=\frac{1}{2}m\omega_0^2(u_\perp^2-u_{||}^2/2+u_{||}^4/R^2+R^2/16), \tag{3}$$

where *m* is the *C*-particle mass, ω_0 is the frequency of its motion in the reactant (product) well, $\mathbf{r}_A$, $\mathbf{r}_B$, and $\mathbf{r}_C$ are the position vectors of the three particles, and $R=|\mathbf{r}_B-\mathbf{r}_A|$ is the *A-B* distance. The $u_{||}$ and $u_\perp$ terms determine the motion of the light particle along the *R* axis and in any transverse direction, respectively (see Fig. 2). In particular, $u_{||}$ turns out to be a suitable choice for the reaction coordinate. Indeed the motion of the light particle along **R** is determined by a symmetric bistable potential (described by the quartic polynomial in $u_{||}$); each well (at $u_{||}=\pm R/2$) corresponds to a stable species with *C* bound to one of the two heavy atoms. The two wells are separated by a maximum (at $u_{||}=0$) representing the barrier to transfer, given by

$$V_0=\frac{1}{32}m\omega_0^2R^2. \tag{4}$$

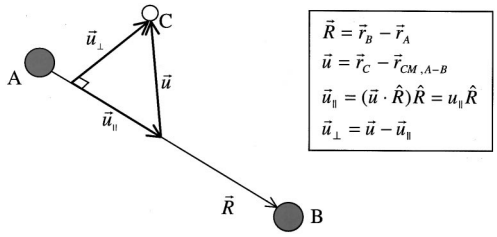

FIG. 2. The *A*-*C*-*B* reaction complex and the various coordinates appearing in the three-body potential, Eq. (3).

The height of the barrier increases as the reactants move apart, but as strong harmonic forces prevent their definitive separation [see also Eq. (5) below], the mean barrier height is well approximated by putting $R=\sigma_{A-B}$ in Eq. (4). The motion of the light particle in the direction normal to **R** is subject to a harmonic restoring force due to the $u_\perp$ quadratic term in the three-body potential. The last term in Eq. (2) is an attractive term added in order to prevent large separations of the two heavy particles:

$$V_R = aR^2. \tag{5}$$

The a constant was fixed at 1.415 kJ Å^{-2} mol^{-1}; with this high value the two heavy particles never separate by more than 6 Å , thus we can always consider the system as a ''tightly bound'' complex.

If we allowed greater *A*-*B* separations the transfer probability would clearly decrease as the two heavy particle must get close before exchanging the *C* species. Working on a ''tightly bound'' complex allows a high number of meaningful (reactive) events to be recorded in a shorter simulation time and at the same time it makes more evident the effect of activation of the reactants with respect to their relative diffusion (which is less interesting in the present study, as remarked before). The flexibility of zeolite framework was accounted for by a nearest-neighbors harmonic model;[26] only the interactions of the guest species with the zeolite oxygen atoms were considered in the simulations. The simulation time step was 1 fs.

The chemical reaction shown in Eq. (1) can be schematized as $A \Leftrightarrow B$; it can be described by the phenomenological rate equations:

$$\dot{c}_A(t) = -k_f c_A(t) + k_b c_B(t) \tag{6}$$

and

$$\dot{c}_B(t) = -k_b c_B(t) + k_f c_A(t), \tag{7}$$

where k_f and k_b are the forward and reverse rate constants respectively, while $c_A(t)$ and $c_B(t)$ denote the instantaneous concentration of species *A* and *B*. Similar rate laws can be written for the fluctuations from equilibrium concentrations $\Delta c_A(t)$ and $\Delta c_B(t)$; if the number of particles is conserved $(\Delta c_A(t) + \Delta c_B(t) = 0)$ one then finds

$$\Delta\dot{c}_A(t) = -k_f \Delta c_A(t) - k_b \Delta c_A(t) = -k \Delta c_A(t), \tag{8}$$

where $k = k_f + k_b$, $\Delta c_A(t) = c_A(t) - \langle c_A \rangle$, and $\Delta c_B(t) = c_B(t) - \langle c_B \rangle$. The solution of the rate Eq. (8) yields

$$\Delta c_A(t) = \Delta c_A(0) \exp(-kt). \tag{9}$$

Equation (9) describes the relaxation of small nonequilibrium perturbations in the concentration of reactants; on the basis of the fluctuation-dissipation theorem, in a system close to equilibrium (linear regime) the decay of such externally prepared deviations from equilibrium coincides with the decay of the correlation between spontaneous thermal fluctuations:[9,27,28]

$$c(t) = \frac{\langle \delta n(0)\, \delta n(t) \rangle}{\langle (\delta n)^2 \rangle} = \frac{\Delta c_A(t)}{\Delta c_A(0)}, \tag{10}$$

where $n(t)$ is a dynamical variable strictly related to $c_A(t)$ and $\delta n(t) = n(t) - \langle n \rangle$. With $q = u_{||}$ as the reaction coordinate ($q=0$ on the barrier, while $q<0$ corresponds to one species and $q>0$ to the other one), the dynamical variable $n(t) = \theta[q(t)]$ [where $\theta(x)$ is the Heaviside function] may be used to distinguish the two species (each one laying within one side of the bistable potential). Therefore, from Eqs. (9) and (10), the normalized autocorrelation function of the fluctuations of $n(t)$ should decay exponentially to zero with a time constant τ_{rxn} equal to the inverse of the rate constant k:

$$c(t) = e^{-t/\tau_{\text{rxn}}} \quad \text{for} \quad t > \tau_{\text{mol}}. \tag{11}$$

This connection allows one to extract kinetic data from an equilibrium simulation by exploiting the spontaneous fluctuations of the variable $n(t)$;[29] this approach is suitable for any activated process that shifts the reactive system between two primary regions of stability. Note that Eq. (11) is valid after a transient time τ_{mol} because the phenomenological Eqs. (6) and (7) cannot be right at very short times. The time τ_{mol} is the characteristic time needed for the transition *after the activation*: its timescale is that of the molecular internal motions that allow the reaction coordinate to thermalize. During this time the excess potential energy of the reaction coordinate is being transferred to the other internal degrees of freedom and to the external environment. On the other hand, τ_{rxn} is the time needed in order to reactivate the reaction coordinate starting from reactants at equilibrium, i.e., the actual average time required for a complete transition from a stable, equilibrated, species to the other one.

The transition state theory (TST) approximation to k may be evaluated by the short time gradient of $c(t)$:

$$k_{\text{TST}} = -\frac{dc}{dt}(t \to 0_+). \tag{12}$$

It can be shown[28] that Eq. (12) is equivalent to the Wigner's assumption that every trajectory which crosses the transition state with positive velocity (i.e., directed towards the products) will always lead to the products, without recrossing the barrier before the complete deactivation. This assumption can break down, for example, if the environment hinders the barrier passage through frequent collisions with the activated complex in the transition state domain.[15] The activation step preceding the barrier crossing and the dissipation of the excess potential energy following the passage, which also influence the ''true'' reaction rate and its deviations from the TST approximation, are strongly connected to the solvent action. A decrease of k compared to k_{TST} could be caused by a very low coupling between the reaction coordinate and its surroundings. For example, if no dissipation occurs shortly

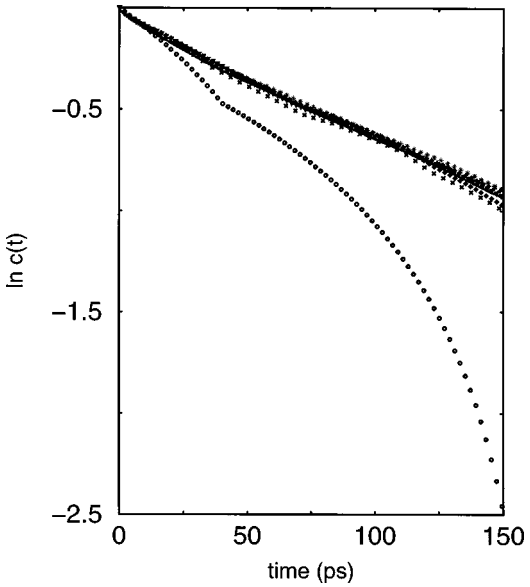

FIG. 3. Logarithmic plots of the $c(t)$ correlation functions calculated by MD trajectories (silicalite, barrier height$=5k_BT$) of different time length τ. Circles: $\tau=1$ ns; crosses: $\tau=4$ ns; other symbols: 5 ns $<\tau<40$ ns.

after the passage in the products well the reaction coordinate will recross the transition state and many recrossings will be observed. Other effects[15,30] can further complicate the overall picture, such as the intramolecular coupling between the reaction coordinate and other internal, non reactive degrees of freedom or the sharpness of the potential curve in the transition region, etc. If the barrier crossing was immediate and no recrossings occurred then Eq. (11) would be valid also in the short-time region, i.e., the relaxation function would decay as a single exponential and the rate constants in Eq. (11) and Eq. (12) would obviously coincide. In other words TST corresponds to assume a single-exponential relaxation of $c(t)$ at all times. The rate constant calculated by Eq. (11) is the ''true'' constant in the sense that it takes into account the possible effect of all the above-mentioned phenomena on the overall transition rate, giving an estimate of its right value to be compared with the TST approximation.

The effect of increasing the barrier height V_0 was firstly examined. By varying the ω_0 parameter V_0 was increased from the low $2k_BT$ value to the more significant $5k_BT$. It must be remarked that longer trajectories are needed for higher V_0 values because the number of significant events (i.e., barrier crossings) decreases with higher barriers. A $c(t)$ function smoothly decaying to zero is needed in order to get an accurate fit of Eq. (11): the rate constants were calculated by the slope of a logarithmic plot of $c(t)$. The transient, short-time part of the log-plot was not included in the fitted region. The statistical accuracy of the obtained values of k can be tested by comparing the log plots of the $c(t)$ functions computed from trajectories of different length. For this purpose we report in Fig. 3 the partial results of a 40 ns run in silicalite with $V_0=5k_BT$. The logarithms of the correlation functions computed from increasingly longer portions of the overall trajectory are shown. The slope of the plots converges to a constant value after 5 ns only; in other words, for the system under study, a trajectory of 5 ns seems to be long enough to give an accurate rate constant in the worse (highest barrier) case. However, in order to further reduce the errors in the computed k considerably longer trajectories were carried out. MD runs of 10, 20 and 40 ns were carried out for $V_0=2k_BT,3k_BT$ and $5k_BT$, respectively. The error present in the calculated values of the rate constants (estimated from a block analysis of data[31]) turns out to be less than 10% for the $5k_BT$ barrier case which, giving rise to the lowest number of crossings, should be affected by higher errors than the other cases.

The adopted procedure is different from the standard ''reactive flux'' method to obtain the rate constant for an activated process[9,32] that has recently been applied to the study of slow diffusive motions in zeolites.[33–36] For activated processes involving very high barriers this is the only suitable method because it would be impractical to follow a single long trajectory spanning several τ_{rxn} to obtain an accurate $c(t)$. Nevertheless we found that, for barriers up to $5k_BT$ and for the reaction complex model adopted, following a single equilibrium trajectory for fairly long times is a very simple and direct way to obtain both the true rate constant and its TST approximation. From Eqs. (11) and (12) it appears that the connection between the $c(t)$ function and the reaction kinetics provides all the information pertaining to the true rate (τ_{rxn}) and to the crossing dynamics (τ_{TST}). The study of the relaxation of $c(t)$, taking into account recrossings and any kind of dynamical processes involved in the transfer reaction, provides information unavailable from a direct inspection of the trajectory, thus representing a suitable and accurate procedure for the present case.

RESULTS AND DISCUSSION

The length of the simulations carried out ensures that the configurational space is adequately sampled; the reactive system explores the two sides of the bistable potential according to a near-Boltzmann distribution. Due to the symmetry of the potential, in an equilibrated system some properties must be fulfilled: we indeed verified that $\langle n(t)\rangle\sim 0.5$ in all simulations and the number of crossings in either direction is practically the same (the direct and reverse rate constants are equal to one-half of the overall k). The symmetry of the system also entails that the k_{TST} calculated by Eq. (12) exactly matches the value calculated according to

$$k_{\mathrm{TST}}^{\mathrm{BC}}=\frac{2N_{\mathrm{BC}}}{\tau_{\mathrm{RUN}}}, \tag{13}$$

where N_{BC} is the total number of barrier crossings and τ_{RUN} is the simulation length.[7] As TST assumes that every barrier crossing actually leads to reaction the direct (or reverse) rate constant in such approximation is given by $N_{\mathrm{BC}}/\tau_{\mathrm{RUN}}$. The inverse of the latter ratio represents the mean lifetime of the *A*-*C* or *B*-*C* species, therefore Eq. (13) corresponds to what reported in Ref. 7: for the studied system $\tau_{\mathrm{TST}}=k_{\mathrm{TST}}{}^{-1}$ is given by half of the mean lifetimes in either well.

The $c(t)$ functions obtained for the $2k_BT$, $3k_BT$, and $5k_BT$ barrier heights are shown in Figs. 4(a)–4(c); the logarithms of $c(t)$ are plotted in the insets. Table I reports the rate constants resulting from the various simulations. In the

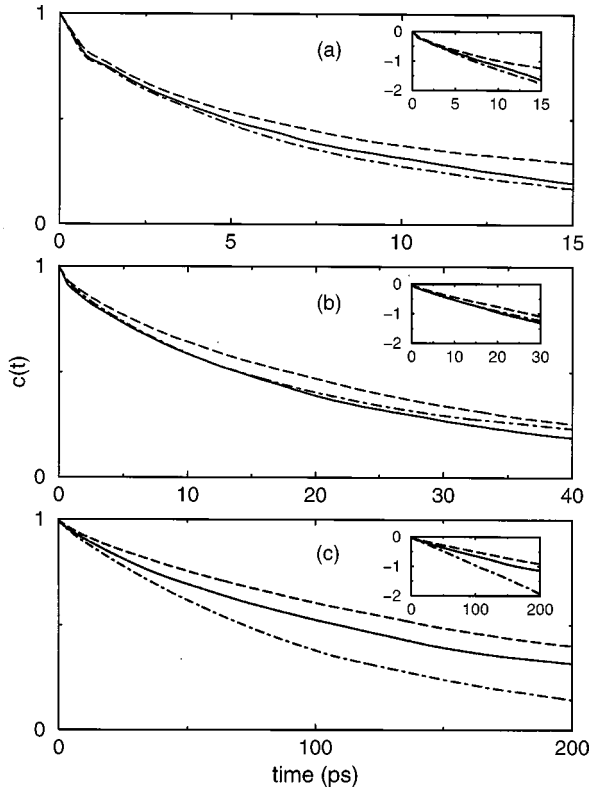

FIG. 4. Normalized correlation functions [Eq. (10)] for the different barrier heights studied. (a): $V_0=2k_BT$; (b): $V_0=3k_BT$; (c): $V_0=5k_BT$. Dashed line: ZK4; continuous line: silicalite; dotted-dashed line: CCl_4. The insets show the logarithm of the $c(t)$ functions. Note the different scales on the time axes.

first column of Table II the total numbers of observed transfers, or barrier crossings, are shown. This value includes all crossings, i.e., a sequence of n close crossing-recrossing events is counted n times. In the second column of Table II any such sequence is grouped to count it as a single event only; in the third and fourth columns the number and the percentage of crossings which do not immediately recross the barrier after shortly visiting the product side are reported (in this symmetric process both the forward and reverse reactions are identical and the term ''product'' can be referred both to *A*-*C* or *B*-*C* species, depending on the direction of the first barrier crossing). A non-recrossing event was defined as a barrier passage neither immediately preceded nor followed by another (re)crossing; we will term it ''TST'' event as it

TABLE I. Rate constants (ns^{-1}).

	Silicalite	ZK4	CCl_4	Silicalite[a]	ZK4[a]
k					
$V_0/k_BT=2$	94.2	73.1	110	-	-
3	38.9	31.8	37.8	49.2	35.9
5	5.5	4.3	9.4		
k_{TST}					
$V_0/k_BT=2$	275	245	297	-	-
3	135	105	123	126	118
5	25	18.7	24.4		

[a]Simulations with stronger guest-host LJ interactions, see text.

TABLE II. Analysis of barrier crossings.

	Total barrier crossings[b]	Net events number[b]	TST (nonrecrossing) events[b]	% TST events	Average number of crossings per event
silicalite					
$2\ k_BT$	1371	520	236	45.4	2.64
$3\ k_BT$	675.5	278	136.5	49.1	2.43
$5\ k_BT$	124	61.5	35.2	57.3	2.01
(a)	630	313	159.5	51.0	2.01
ZK4					
$2\ k_BT$	1223	471	203	43.1	2.60
$3\ k_BT$	529	256	131	51.2	2.07
$5\ k_BT$	93.7	52	31	59.6	1.80
(a)	589.5	311.5	169.5	54.4	1.89
CCl_4					
$2\ k_BT$	1486	547	238	43.5	2.72
$3\ k_BT$	612.5	298	150	50.3	2.05
$5\ k_BT$	121.2	71.5	44.5	62.2	1.69

[a]Simulations with stronger guest-host LJ interactions, see the text.
[b]Normalized to 10 ns.

corresponds to the transition state theory assumption. A sample TST trajectory is shown as the dashed curve in Fig. 5 while the solid curve is representative of a typical recrossing event. We see that, after crossing the barrier and reaching the repulsive wall of the product side, in the non-TST case the reaction coordinate is directly driven back to the reactant side while in the other case it quickly thermalizes. The recrossing time is $\sim$ 1 ps. The distinction made between TST and non-TST events is useful to understand some qualitative features of the reaction on the basis of the observed percentages of TST events (see below), but it could not be directly and quantitatively associated to the rate constants k in Table I. The latter are the exact values, as shown above, because the decay of the $c(t)$ function is controlled by many events

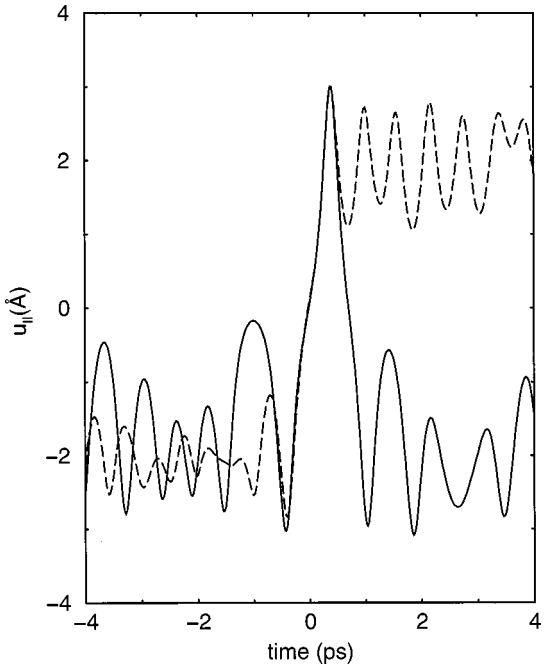

FIG. 5. Reaction coordinate profile for a ''TST'' barrier crossing (dashed line) and for a recrossing event (solid line).

that cannot be easily accounted for with a simple definition of TST crossings. The latter numbers only represent a rough estimate of the *real* number of reactant-product transitions that could give the exact k values through an expression analogous to Eq. (13). Indeed, the k calculated through the number of TST crossings underestimate the values of Table I for $2k_BT$ and $3k_BT$ barriers while for $V_0=5k_BT$ the exact rate constants are overestimated. The discrepancy arises from the definition of TST event and in particular from the arbitrary choice of the time interval without recrossings. The ''no-recrossing'' interval has been chosen to be 4 ps: this is slightly longer than the average recrossing timescale, but shorter than the reaction time τ_{rxn} in all cases. The first requirement excludes from the TST crossing number those transitions in which the recrossing occurs slightly later than the average; the second point is important to distinguish between recrossings and actual reactions. There are mainly two source of error in this definition: (a) if a barrier crossing is followed by just two (or any even number) quick recrossings, the net result is a reactant-product transition, but one not included in the overall TST crossing number while still contributing to the decay of $c(t)$ and thus affecting the k value; (b) the recrossing can occasionally occur shortly after the 4 ps limit since the first passage. When the rate constant is evaluated from the TST crossing number the (a) events cause an underestimation of k, while the (b) cases determine an overestimation. It thus seems that the weight of (b) events is greater for the highest barrier, while the (a) events dominate for the two lower barriers. It is not easy to verify these points, or to give a more accurate definition of TST event based for example on a time interval different than 4 ps for the recrossings, because of the distinct reaction times τ_{rxn} for each barrier height. For instance, after increasing the time limit for the recrossings to 16 ps, the recalculated number of TST crossings gives a better estimate of k for $V_0=5k_BT$; nevertheless the same time limit is not suitable for the lower barriers because it would overlap with the time scale for the reaction ($\tau_{\mathrm{rxn}}\sim 182$ ps for $V_0=5k_BT$ in silicalite, but it falls to 26 ps for $3k_BT$, and ~ 11 ps for $2k_BT$). Another improvement could arise by including all the transitions with an even number of passages in the TST crossing number but this would be complicated by the longer time needed for the transitions characterized by more than one crossing, which should be taken into account in some other way. All these effects are automatically included in Eq. (11) and there is no need of further efforts to get a more accurate TST crossing number. The numbers of Table II will only be used for a qualitative comparison between different environments.

The reaction rates shown in Table I decrease with higher barriers following a linear, Arrhenius-type, behavior when $\ln(k)$ is reported vs V_0/k_BT (filled symbols in Fig. 6); actually the curves in the zeolites are almost parallel, while CCl_4 shows a more irregular trend, with a rate constant falling just below the silicalite one only for $V_0=3k_BT$. The transition-state approximated constants show a more linear trend than the effective constants (open symbols in Fig. 6). In all cases ZK4 appears to be the least effective environment in promoting the atom transfer. The rate constants in silicalite are always closer to those obtained in CCl_4 and only for the highest $5k_BT$ barrier the liquid definitely appears as the most effective environment (Table I and Fig. 4). Since with the present model the long-range diffusional approach of the reactants has little influence on the reaction rate, the observed different rates in the two silicates are mainly due to their different effectiveness in the activation–deactivation of the reaction coordinate. Some factors could determine this different efficiency: notwithstanding the potentials describing all inter- and intramolecular interactions are identical, the internal vibrational modes of the two silicates show differences due to the different crystal structures. This is evident from the vibrational spectra reproduced by the present harmonic model.[5] Therefore the guest-host vibrational coupling could determine a more effective energy exchange between the reaction coordinate and the silicalite framework. In order to check this hypothesis the total energy along the reaction coordinate, defined as

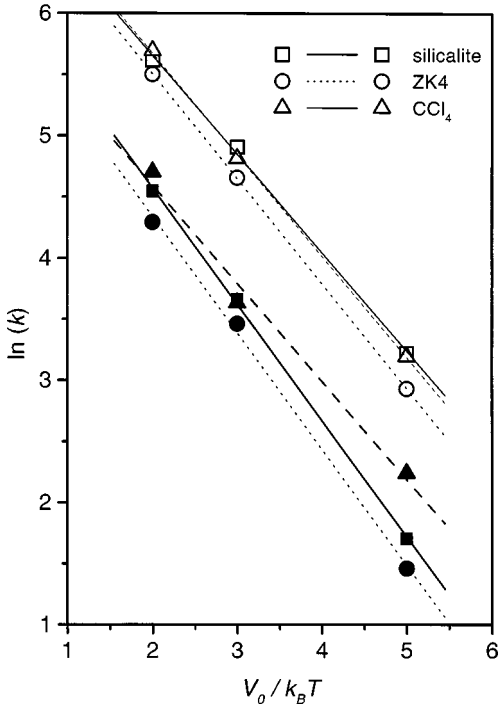

FIG. 6. Arrhenius plots of the data in Table I. Full symbols represent ''true'' rate constants [Eq. (11)], open symbols TST approximated values [Eq. (12)].

$$E(t)=V[u_{||}(t)]+\frac{1}{2}m\dot{u}_{||}^2(t) \tag{14}$$

has been averaged over all ''TST'' crossings. The first term in Eq. (14) is the potential energy along the reaction coordinate [retaining only the $u_{||}$ terms of Eq. (3)], and the second term is the corresponding kinetic energy. The non-TST events have not been included in the average because they would complicate the interpretation of the energy curves. We found more convenient to include in the averaged ensemble only the TST events because they are *isolated* and then uncorrelated from each other, thus better representative of a typical barrier passage. Moreover such events have a higher statistical weight in the ensemble including all crossings: they always directly lead to the products, thus giving the

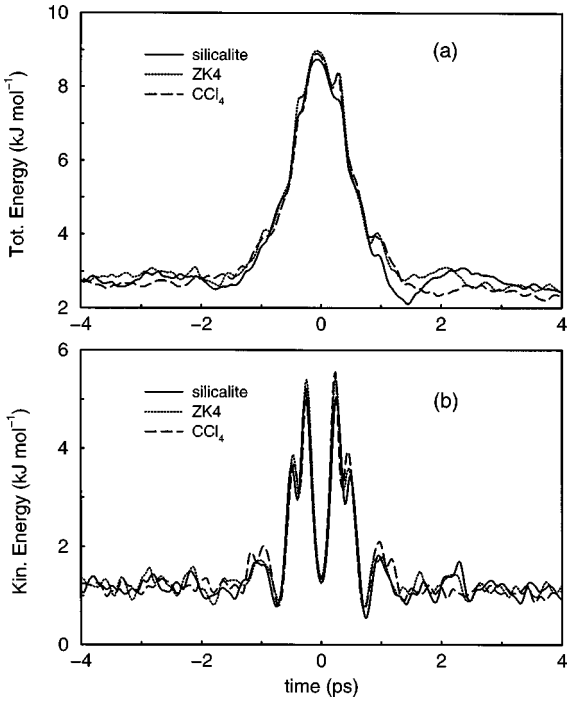

FIG. 7. Total (a) and kinetic (b) energy of the reaction coordinate averaged over all nonrecrossing transitions for the $V_0=3k_BT$ case. $t=0$ corresponds to the crossing of the barrier.

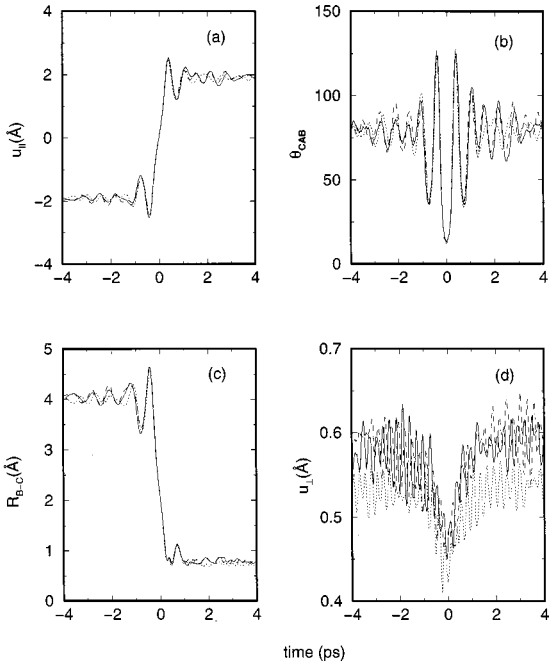

FIG. 8. Some geometrical properties of the reactive complex averaged over all nonrecrossing transitions for the $V_0=3k_BT$ case. (a) Reaction coordinate $u_{||}$; (b) $\angle$ *C-A-B* angle (in degrees); (c) *B-C* distance; (d) $u_{\perp}$ coordinate, describing the perpendicular distance of the *C* particle from the *A-B* axis. Note that the reactant and product species are *A-C* and *B-C*, respectively. Continuous lines: silicalite; dashed lines: ZK4; dotted lines: CCl_4.

most important contribution to the rate constants. Figure 7 shows the average total and kinetic energies for the $V_0=3k_BT$ case. The trend observed in the three environments is very similar: the transfer process starts less than 2 ps before the crossing (this is more evident from the developing oscillations in the kinetic energy curves and from the trend of some geometrical properties of the reactive complex analyzed below), then the three curves are practically superimposed 1 ps before and after the crossing. The same similar behavior is also observed for the other barrier heights examined. Therefore the differences between the reaction rates in the two silicates cannot be ascribed to a faster energy transfer in silicalite. The rate at which the *activated* complex climbs the energy barrier along the reaction coordinate and then transfers the excess energy into the other degrees of freedom is roughly the same in all ''solvents.'' Moreover, if also the geometry of the *A-C-B* species is studied during the reactive crossings, we can conclude that the transfer mechanism is practically unchanged in the three environments. Indeed Fig. 8 shows that the main features of the transfer are the same in all cases. Note that the extensive averaging over many crossing trajectories considerably smoothes out the oscillations of the reported parameters due to their different phase [look, for example, at the differences between Fig. 5 and Fig. 8(a)]. The averaged curves give also some insight into the transfer mechanism, together with the direct inspection of the computer-animated evolution of some selected MD trajectories near to the transition. While the *A-B* dumbbell is slowly oscillating around the equilibrium distance the *C* particle quickly rotates around the *A* one, and during this rotation it continuously moves from the ''internal'' region between *A* and *B* (corresponding to the lower values of the $\angle$ *C-A-B* angle) to the external region at greater angles. This is clearer in Fig. 9, where the angle in a sample *single* trajectory is shown. Figure 8(b) shows that the $\angle$ *C-A-B* angle is minimum at $t=0$ indeed the transfer usually occurs after the light particle has moved to the internal region, almost aligned to the *A-B* axis. The dynamics of the transfer can be roughly

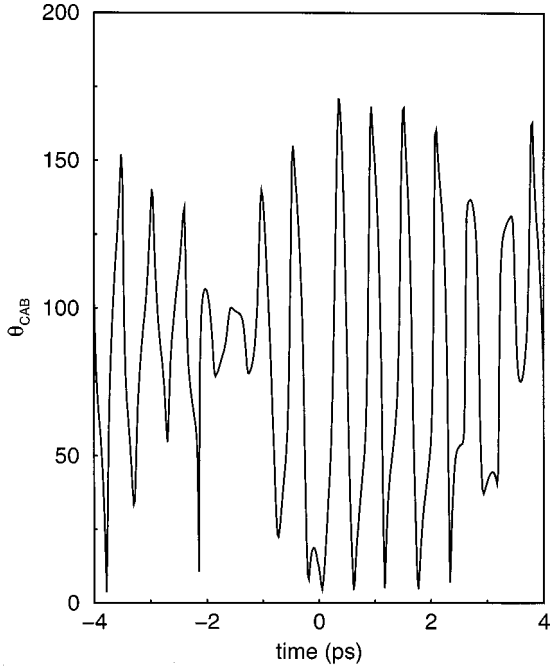

FIG. 9. Evolution of the $\angle$ *C-A-B* angle (in degrees) for a *single* reactive crossing: note the probable occurrence of a collision with the host at $t=-2$ ps.

TABLE III. Arrhenius parameters.[a]

	Silicalite	ZK4	CCl_4
A (ns^{-1})	649±8	515±12	492±26
$E^{\neq}/V_0$	0.95±0.02	0.95±0.03	0.80±0.09

[a] $k = A \exp(-E^{\neq}/k_B T)$.

TABLE IV. Analysis of the barrier crossing locations in silicalite; values in parentheses are the overall time fractions spent in each region.

	% Straight channel	% Zigzag channel	% Intersection
$V_0/k_B T = 2$	23.3(24.7)	34.6(38.1)	42.1(37.2)
3	23(22.7)	33.3(39.2)	43.7(38.1)
5	22.8(23.9)	40.0(39.5)	37.1(36.6)

described in this way: following the activation the *A*-*C* bond starts to oscillate with higher amplitudes and on each next rotation that brings the *C* species in the favorable region between *A* and *B*, *C* gets increasingly closer to *B* (look at the minimum at −0.8 ps in Fig. 8c) until the *A*-*C* bond can be broken and the *B*-*C* species is almost simultaneously formed. It is interesting to note that the activated complex, taken as the geometry adopted at $t=0$, is almost linear: the *C*-*A*-*B* angle is at a minimum of 15° (Fig. 8b) and the normal distance $u_\perp$ from the *A*-*B* axis converges to a minimum at $t=0$ [Fig. 8(d)]. Moreover the only (slight) difference in mechanism between the three environments can be seen in the evolution of $u_\perp$: in CCl_4 the *C* species is kept closer to the axis connecting the heavy particles and the transition state configuration is a little more compact than in the silicates.

The energy curves in Fig. 7 and the described mechanism are representative of the crossing events only, i.e., they show that, once the reaction coordinate is activated, the following dynamics is mostly independent on the environment. However, they could not take into account the longer time interval (on the order of τ_{rxn}) between the reactive events, i.e., the time needed to ''prepare'' the atom transfer. The action of the environment on this time scale mainly affects structural and equilibrium properties that should then be crucial in determining the observed differences. The faster transfer rate in silicalite probably stems from a higher activation *frequency*: the time needed to reactivate an equilibrated species should be shorter than in ZK4. This seems to emerge from both the k_{TST} values in Table I and the (net) crossing numbers in Table II, which are always higher in silicalite. Indeed, the almost constant percentage of TST events (with fixed V_0) in all environments confirms that none of them is more effective in favoring the thermalization of the excited reaction coordinate after the barrier passage, i.e., in preventing the recrossings. Therefore a higher number of ''attempted transitions'' (net events in Table II) will presumably lead to higher rate constants as the probability of success is roughly constant. Moreover looking at the Arrhenius parameters for the straight fits to the log plots in Fig. 6, reported in Table III, we see that, while the *effective* activation energy is the same in the two zeolites, the preexponential term is considerably higher in silicalite, presumably reflecting the higher ''collision frequency'' between the reactants which ultimately leads to the higher number of transfers. While the logarithmic curves in the two zeolites are fairly linear and then easily comparable, the Arrhenius parameters in the liquid solvent are affected by higher errors. However, within the error bars, the activation energy in CCl_4 is about 20% lower than V_0 while the zeolites shows a decrease of only 5%. While V_0 is the *potential* energy barrier to transfer, i.e., the gas-phase activation energy depending only on the intramolecular interactions, the *effective* barrier is usually altered by the additional contribution of the environment.[37] Thus in the liquid solvent the *static* contribution changing the relative energies of reactive species (both at the bottom of the potential wells and at the barrier top) seems to be more important than in zeolites. In other words, for this model reaction the liquid is probably more effective in lowering the energy barrier compared to the zeolitic environments. This effect could also be connected to the more compact arrangement of the transition state in CCl_4 highlighted above.

Next we have to explain *how* the silicalite structure can favor a higher number of transitions than ZK4. In the former the reaction complex moves along straight and zigzag channel sections and their intersections, thus experiencing significantly different environments, each one imposing different constraints to the reaction. This can in principle lead to multiple rate constants[38] whose mean values are probably those shown in Table I. ZK4 offers a more uniform and less confining environment to the reactive event, consisting of large cages (whose dimensions are even larger than the channel intersections in silicalite) connected by very narrow windows with diameter not much greater than that of the *A* and *B* particles. This structural difference should be the main source of the different behavior observed in this particular process. In order to elucidate the influence of specific regions on the reaction the transitions occurring in silicalite were divided on the basis of a map recently devised by us,[39] which allows to identify the region (straight channel, zigzag channel or intersection) visited by the sorbate at a particular time. We mapped the position of the *A*-*B* center of mass (again for the TST crossings) whenever $u_{||}$ changed sign. At that time the *A*-*B* center of mass is close to the position of the transferring *C* species: indeed, at the transition state, the distances of *C* from *A* and from *B* are roughly equal and the *A*-*C*-*B* arrangement is almost linear, as seen before. The percentage of crossings found in each region is reported in Table IV; the values in parentheses are the fractions of the whole trajectory spent in the same region. From the reported data it seems that the distribution of reactive events in silicalite is mainly statistic: the fraction of crossings occurred in each region mostly reflects the time fraction spent there by the reaction complex. If a specific region favored the transfer reaction the percentage of events found in that region would be *higher* than the fraction of time spent there. We see that, for the straight channel, the two percentages are always identical, while (for barrier heights of $2k_B T$ and $3k_B T$) the intersections seem more favorable for the reaction compared to the zigzag channels. However the differences are small and completely disappear for the highest barrier. Therefore the fact

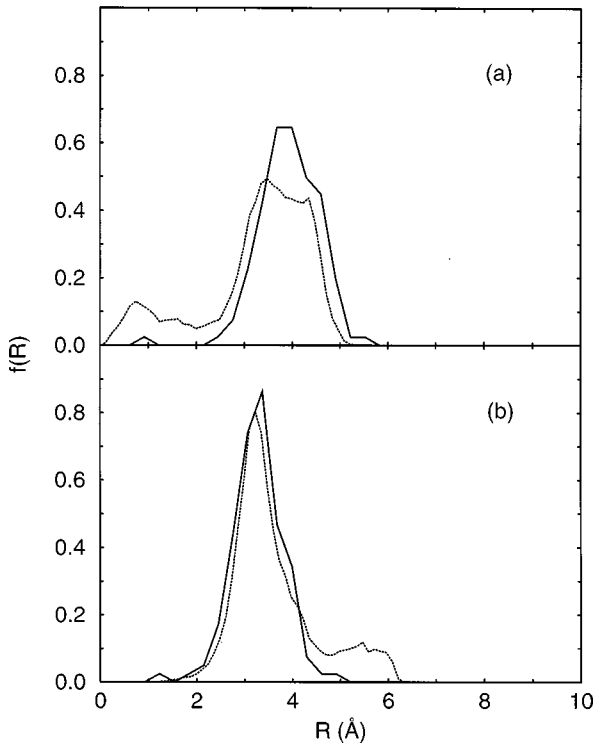

FIG. 10. Distribution of the positions of reactive crossings (solid lines) and of the whole trajectory (dotted lines) with respect to (a) the closest window center; (b) the cage center, for the ZK4 run with $V_0=3k_BT$.

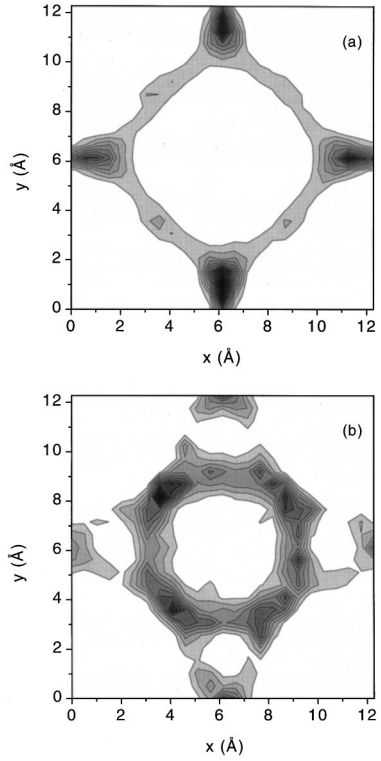

FIG. 11. Projections on the *xy* plane (at $z=L/4$) of the three-dimensional distribution function of (a) the coordinates of $A(B)$ species, (b) the *A-B* center of mass coordinates, for the ZK4 run with $V_0=3k_BT$. Darker areas correspond to higher density regions.

that the reaction complex spends more time in the channels than in the intersections (about 62% of the full trajectory) is presumably not the reason of the higher reaction rates in silicalite because in the intersections the reaction occurs with the same, if not higher, probability. Turning to the ZK4 case we calculated the distributions of reactive events and of trajectory points located at a particular distance from the center of the (closest) window [Fig. 10(a)] and from the cage center [Fig. 10(b)]. In the first case the main difference between the two distributions is the absence of reactive crossings in the region near the windows, where the reaction complex spends a non negligible fraction of time, albeit lower than the time spent in the cage (the main maximum in the figure). Fig. 10(b) shows the same phenomenon from another point of view: the reaction complex always avoids the cage center and it is preferentially adsorbed 3-4 Å apart, i.e., near the cage walls. The reactive crossings preferentially occur at similar distances from the cage center. However a non-negligible tail at higher distances is present in the trajectory distribution and disappears in the distribution of reactive crossings. This tail corresponds again to the region near the windows, which seems to be definitely unfavorable for the transfer reaction. In order to further investigate this point the three-dimensional distribution functions[40] of both the *A-B* center of mass and of single *A* (and, equivalently, *B*) species in the zeolite cavities were calculated. For ZK4 one eighth of the unit cell containing exactly one cage at its center was divided in $25\times25\times25$ small cubes (with side $\sim$ 0.5 Å). The coordinates were reported in this ''subcell'' through inverse symmetry operations and we calculated how many configurations were placed in each cube. The projections of these distributions in the central *xy* plane at $z=L/4$ (i.e., with the cage center in the middle) are reported as contour plots in Fig. 11. It is evident that both the heavy particles tend to be located in the cage, near the window entrances; at least one out of the two is always placed in these sites. Looking at the contour plot of the center of mass positions [Fig. 11(b)] it is clear that the other one can be placed in the same cage, with the *A-B* axis roughly aligned with the cage wall, or in the adjacent cage, with the center of mass placed at the window center (evidenced by the relative maxima at $x,y=L/4$, 0 and 0, $L/4$ in the C.M. contour plot). As seen before the latter arrangement does not allow the *C*-transfer to occur and this presumably is the main reason of the lower transition rates in ZK4. Indeed from the probability distributions of Fig. 10 the fraction of configurations with the *A-B* center of mass placed near the windows can be estimated as $15\div17\%$, to be compared with the $\sim$22% increase in the rate constant going from ZK4 to silicalite ($V_0=3k_BT$).

The further small rate difference in favor of silicalite might denote that also the configurations with the center of mass in the cage of ZK4 are not as favorable as the conformations adopted in silicalite. One hint in this direction comes from the mean interaction energies between the guest reaction complex and the host framework, given by

$$\langle U_{g-h}\rangle=\langle U^{LJ}_{A-h}\rangle+\langle U^{LJ}_{B-h}\rangle+\langle U^{LJ}_{C-h}\rangle. \tag{15}$$

The obtained values, referred to the runs with $V_0=3k_BT$, are $\langle U_{g-h}\rangle=-57.6$ kJ mol^{-1} for silicalite and -38.0 kJ mol^{-1} for ZK4. The *A-C-B* complex is adsorbed much more

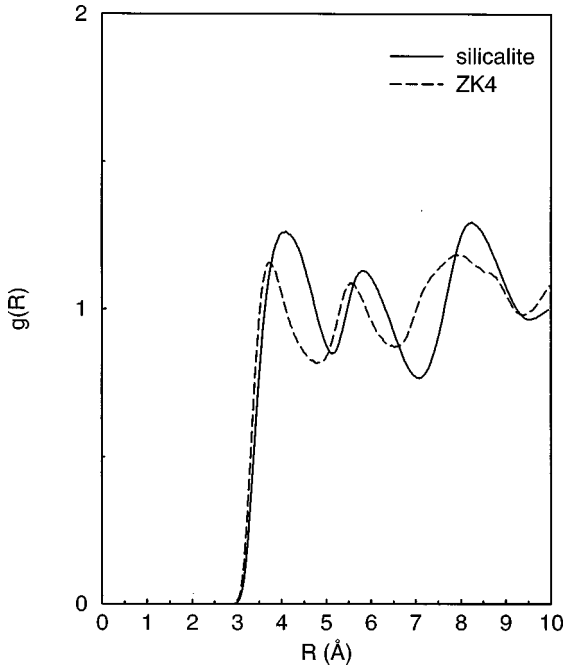

FIG. 12. Oxygen-heavy atoms radial distribution functions for silicalite and ZK4 (runs with $V_0=3k_BT$).

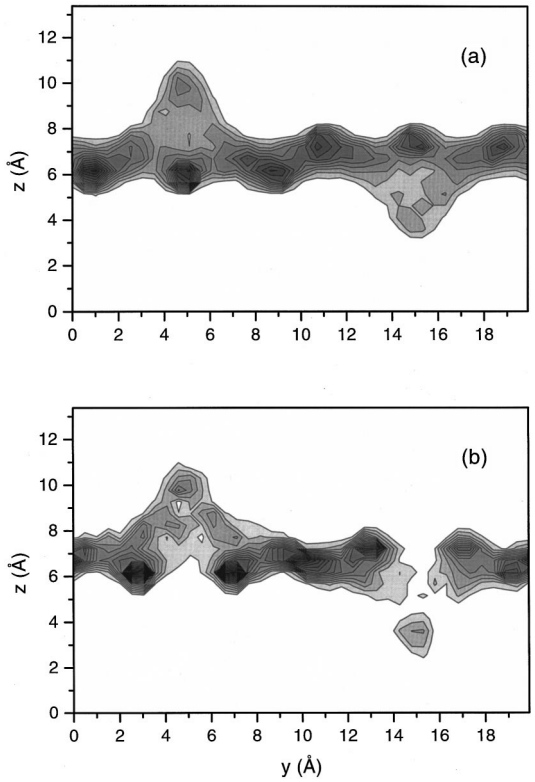

FIG. 13. Projection on the *yz* plane (at $x=0$) of the three-dimensional distribution function of (a) the coordinates of $A(B)$ species, (b) the A–B center of mass coordinates, for the silicalite run with $V_0=3k_BT$. Darker areas correspond to higher density regions.

strongly in silicalite. This is due to the higher number of oxygens that can closely interact with it, in particular in the channels where the molecule is fully surrounded by the interconnected ten-rings of oxygen atoms. In ZK4 the molecule can only interact with the oxygens in the nearest cage wall and the absence of a near opposite wall determines the lower adsorption energy. In fact, the average number of first neighbors oxygen atoms is 15.4 for silicalite and 9.3 for ZK4. These numbers have been calculated by integrating the oxygen-heavy atom radial distribution functions (rdf's) in the 0–5 Å interval, which is the range covered by the first peak in the rdf's shown in Fig. 12.

The contour plots for the silicalite run were calculated by dividing the unit cell in $40\times40\times27$ cubes (so that the side is still $\sim$0.5 Å) and determining how many configurations were placed in each cube. Figure 13 shows a ''slice'' of this three-dimensional distribution corresponding to the straight channel while in Fig. 14 the sinusoidal channel is contoured. In the straight channel some different configurations for the reactive complex are possible. Comparing the distributions of the heavy species with that of their center of mass and remembering that the *A*-*B* distance is always close to 4 Å it seems that the most common arrangements are two: (i) those with one heavy atom in the intersections (located at $y=5$ and 15 Å) and the other in the channel; (ii) the configurations with both atoms in the channel, arranged with the *A*-*B* axis oblique with respect to the channel axis and with the center of mass roughly at the center of the channel. Turning to the distributions in the sinusoidal channel, we see that here only one arrangement is possible, with both atoms placed along the channel and the center of mass located well inside the channel. The results of Table IV showed that while the molecule remains trapped in this arrangement for a rather long time the transfer of the light particle can be slightly ham-

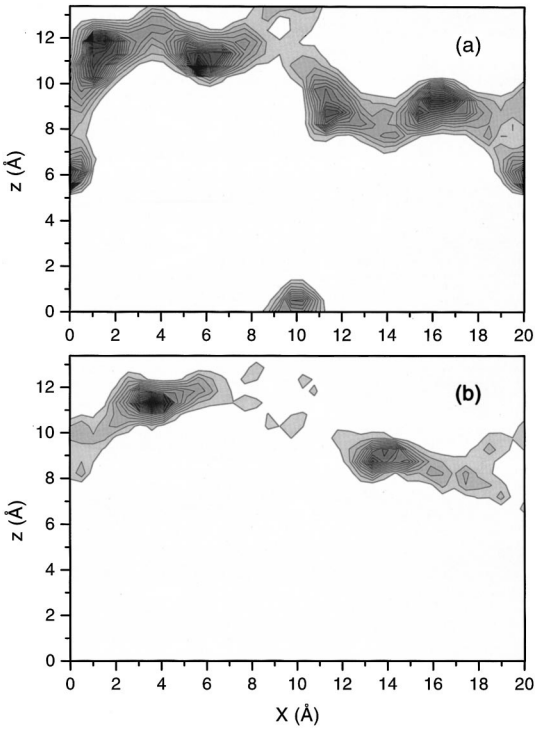

FIG. 14. Projection on the *xz*-plane (at $y=b/4$) of the three-dimensional distribution function of (a) the coordinates of $A(B)$species, (b) the A–B center of mass coordinates, for the silicalite run with $V_0=3k_BT$. Darker areas correspond to higher density regions.

pered, compared to the transfer probability when the center of mass is in an intersection or in the straight channel. This phenomenon, albeit less marked, is similar to the complete absence of transfer events when the center of mass of the molecule is locked in a ZK4 window.

Another important effect has been highlighted by calculating the work done on reactants by the solvent, which is a suitable measure of the guest-host interaction during the reactive event.[16,19,41] The work done by solvent atom i on reagent atom j up to time τ following the barrier crossing (at $t=0$) is

$$w_{ij}(\tau)=\int_0^{\tau}\mathbf{f}_{ij}(t)\cdot\mathbf{v}_j(t)dt, \tag{16}$$

where $\mathbf{f}_{ij}(t)$is the force exerted on the reagent atom j by the solvent atom i, and $\mathbf{v}_j(t)$ is the velocity vector of the reagent atom. The total work done on the reactive complex by the ith solvent atom during the time τ is then

$$w_i(\tau)=\sum_j w_{ij}(\tau), \tag{17}$$

where the index j runs over the three reagent atoms A, B, C. Following each barrier crossing the work $w_i(\tau)$, with $\tau=2$ ps, was determined for each zeolite oxygen i. These atoms were then ranked by their corresponding value of $w_i(\tau)$: atom 1 did the more positive work in the 2 ps following the crossing, while atom 384 did the more negative work. Note that atoms doing positive work are transferring energy to the reactants, while a negative w_i denotes that atom i is removing energy from the A-C-B complex. The ranked work was then averaged over all barrier crossings in silicalite and ZK4 for the $V_0=3k_BT$ case, and it is displayed in Fig. 15 as thin lines. We see that in both zeolites the work done by most oxygens is near zero: only a small fraction of atoms does significant work, both positive and negative. By further examining these fractions, shown in the insets, it results that in silicalite the atoms doing positive work give a larger contribution than the corresponding atoms in ZK4; likewise the work done by the fraction of atoms doing negative work is again larger (more negative) for silicalite. In other words, even though in both zeolites few oxygens are directly involved in the energy transfer after the reaction, the interaction of these atoms with the reagents is more effective in silicalite. This point also emerges from the trend of the cumulative work done by the oxygen atoms, shown as thick lines in Fig. 15: the contribution of the few atoms doing positive work is about $20\ \mathrm{kJ\ mol^{-1}}$ in silicalite, and $13.4\ \mathrm{kJ\ mol^{-1}}$ in ZK4. This difference is counterbalanced by the atoms doing negative work which are again more effective in silicalite. Therefore the total work done on the reagents, i.e.,

$$w(\tau)=\sum_i w_i(\tau), \tag{18}$$

where the index i runs over all oxygens, is similar in both environments. Since we considered the work done in the interval following the barrier crossing, $w(\tau=2\mathrm{ps})$ is negative, corresponding to the energy flux from reactants to the

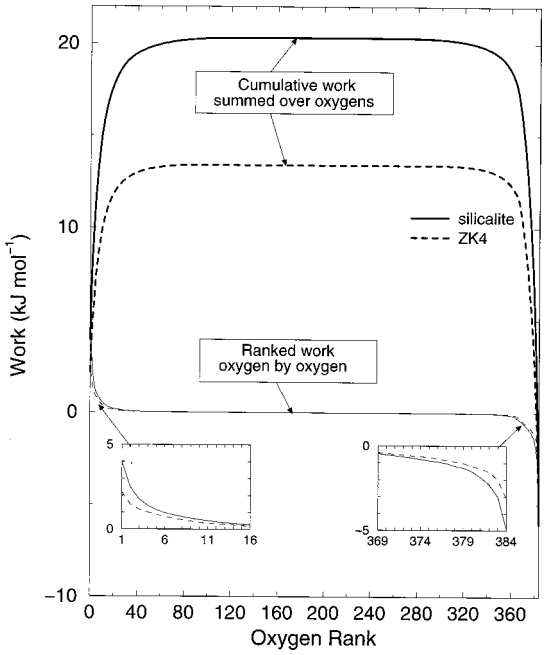

FIG. 15. Thin lines: ranked work done on the reagents by the zeolite oxygen atoms; atoms are ranked according to their maximum value of work done (see text) in the 2 ps following each barrier crossing. The two insets show with higher detail the ranked work done by the 16 atoms doing the more positive and the more negative work. Thick lines: cumulative work done by the oxygen atoms (integral of the ranked work over the oxygens).

environment. The fact that the overall work done on reactants in 2 ps is comparable in the two zeolites reflects the similar trend in the energy curves of Fig. 7(a): the energy removed from the reactive complex after 2 ps is about the same in the different environments. However this seems to arise from the cancellation of the larger positive and negative work contributions in silicalite. On one hand the net result is that close to the barrier crossing the energy transfer occurs with similar rates; on the other hand, the larger efficiency of silicalite oxygens both in accepting and transferring energy to the triatomic may be involved in the higher reaction rates observed on longer time scales.

From the preceding observations it results that the more favorable environment for a heavy-light-heavy particle transfer in the zeolite micropores should be a fairly confining one, in order to maximize the attractive guest-host interactions. When the triatomic molecule resides in the large ZK4 cages its interaction with the zeolitic framework is weaker than in the silicalite cavities. A more effective interaction with the neighboring oxygen atoms, while not directly affecting the short-time rate of energy transfer and the mechanism of the activated process near to the barrier crossing, seems to increase the rate at which the equilibrated sorbate can be reactivated after thermalizing in the products well. At the same time a stronger confinement suppresses the transfer (as in the ZK4 windows and, to a lesser extent, in the sinusoidal channels of silicalite) because a fair rotational freedom is needed for the reaction to occur: the rotations of the vibrationally excited A-C molecule that shift the light particle near the ''acceptor'' B species just before the transfer are hindered in narrow environments. These structural requirements are bet-

ter satisfied in silicalite; in particular when one of the two species is in an intersection both requirements are likely to be fulfilled.

It is interesting to observe that, for the studied process, the liquid solvent definitely turns out to be the most efficient environment only when $V_0=5k_BT$. The *trans-gauche* conformational isomerization of n-butane is an example of activated process with a very similar energy barrier. June *et al.*[38] obtained rates for the isomerization reaction of butane in silicalite considerably lower than in the liquid solvent. This is in agreement with our results with a comparable barrier, notwithstanding the considerable differences in the reactions studied. The authors ascribe such behavior to the hindering on the isomerization process due to the occlusion of the molecule in the narrow silicate pores. Nevertheless for the present transfer reaction (which is made fairly similar to an unimolecular isomerization by the imposed constraints) other effects can come into play in determining the larger efficiency of the liquid solvent. Besides the static effects modifying the relative energies of the reactive species mentioned above, the better matching between the masses of CCl_4 and of heavy xenon-like solute species could also favor the reaction through more effective collisions compared to the two silicates.

Another point emerging from Table I is that TST considerably overestimates the rate constants in all cases (the k_{TST}'s are always 2–4 times larger than the ''true'' constants). This is due to a high recrossing probability, which leads to a decrease of k compared to k_{TST}. Many recrossings may arise when the coupling to the environment is low, in particular with a not too high reaction barrier: the reaction coordinate, after crossing the barrier, retains most of its excess energy, and quickly recrosses the transition state after having visited the products side for a short time ($\sim\tau_{mol}$). We see in Table II (fourth column) that the percentage of nonrecrossing (TST) transitions increases with greater barrier heights in all environments, and the last column shows that the mean number of crossings per single event is a decreasing function of the barrier height. Then a higher barrier correctly leads to a lower recrossing probability, but the tendency to recross the barrier results rather high in all cases accounted for. In the present case the reactive complex *A-C-B* possesses only a few internal degrees of freedom over which the reaction coordinate may distribute its excess energy; thus, in absence of a strong coupling between these non-reactive degrees of freedom and the bath, a great part of the excess activation energy is likely to flow again into the reaction coordinate *before* being transferred to the solvent. If the number of internal degrees of freedom that can equipartition energy with the reaction coordinate on the time scale of the crossing is higher (like, for example, in the isomerization of a polyatomic molecule) then the dissipation could be more efficient even at very low coupling with the solvent.[42–44]

In order to investigate the effect of the coupling to the external bath, two more 20 ns simulations in silicalite and ZK4, with $V_0=3k_BT$, were performed with a three times deeper minimum for the interaction between the zeolite and the two heavy bodies; all the other parameters were left unchanged. This corresponds to a higher ''friction'' exerted by the host (i.e., the attractive forces exerted on the solute are stronger and its translational motion gets considerably slower) and not, strictly speaking, to a more effective guest-host (external) coupling; nevertheless some related information could be gained also in this way.[15] The results are reported in Tables I and II. Compared to the runs with lower intermolecular interactions k increases both for silicalite and ZK4. The higher k values arise from an increased total number of (net) crossings and from a slightly higher percentage of nonrecrossing events. The increase in the rate constants shows the non-negligible influence of the guest-host interactions in this process and confirms that the high recrossing probability observed for this system may be connected to the weak intermolecular coupling. More work is needed to assess the exact nature of its action, which cannot easily be associated with the effects discussed so far. For example the structural properties, such as the distributions in the cavities, considerably change when the attractive guest-host forces are modified and the considerations made above may be no more valid.

TABLE V. Rate constants (ns^{-1}) for the ''loosely bound'' complex simulations.

	Silicalite	ZK4	CCl_4
k	26.2	16.6	26.7
k_{TST}	96	80.9	105.3

Finally we tested the effect of lowering the force constant for the *A-B* interaction to one-half of its previous value. This corresponds to a ''loosely bound'' complex in which the *A-B* distance may reach higher values (up to 7.5 Å). The rate constants, for the runs with $V_0=3k_BT$, are reported in Table V. Compared to the previous rates there is obviously a net decrease as the reactants are on average farther from each other. ZK4 gives rise to the more marked decrease (-90%) followed by silicalite (-50%) and CCl_4 (-30%). It is interesting to note that the further increase in the difference between the rates in the two silicates is not due to a different distribution of the *A-B* distances: as in the previous runs the distributions in silicalite and ZK4 are identical. The overall trend is unchanged with respect to the previous runs with $V_0=3k_BT$: $k_{(ZK4)}<k_{(silicalite)}\sim k_{(CCl4)}$, showing that the general features observed for this process are not heavily sensitive to the *internal* (as opposed to the *external*, or *intermolecular*) parameters adopted, in particular to the choice of a ''tightly bound'' complex. Actually, only if we loosened the *A-B* bond at the point that a CCl_4 molecule could easily slip between the heavy atoms (which would require *A-B* separations of almost 10 Å) we would obtain considerably different rates in the liquid solvent. But in such case the dynamics of the transfer would significantly differ from the process studied so far: the reactants might considerably separate from each other and their relative diffusion would affect the rates. Moreover such simulations would require very long MD runs in order to observe a fair number of transitions and the application of the present method is no more suitable.

CONCLUDING REMARKS

In this paper we analyzed the influence of three different environments on the model of an activated transfer reaction proposed by Allen and Schofield. The triatomic model provides a convenient description of the microscopic dynamics of breaking and formation of bonds, yet most of the relevant correlations are intrinsically present. The fact that the reactant are always kept close to the reaction distance through harmonic restoring forces facilitates not only the simulations but also the analysis of the reactive paths in such environments.

It has been shown that useful information concerning the dynamics and the kinetics of activated transfer processes in zeolites can be obtained from a standard correlation functions analysis applied to classical equilibrium molecular dynamics trajectories, as long as the energy barrier separating reactants and products is not too high. The small size of the light *C* particle compared to the heavier *A*-*B* ones mainly reduces the problem to the interaction of the *A*-*B* substrate with the environment. The diffusional constraints imposed on the relative *A*-*B* motion further emphasize the importance of the coupling between these masses and their surroundings.

The adopted model is also a suitable tool to test the basic assumptions that are made in the TST approximation. It is known that standard TST, when applied to a heavy-light-heavy particle transfer reaction, may be seriously in error: the rapid motion of the light particle within the force field of the two slowly moving substrate species leads to considerable recrossings of the transition state.[37] We indeed verified such behavior: the actual rate constants measured are considerably lower than their TST estimates. Further insight into the barrier crossing dynamics has been obtained through a direct computation of the number of effective (TST) crossings in each case.

The main point emerging from the simulations is the greater effectiveness of silicalite in the activation of reactants, as compared with ZK4. The rate constants in the latter environment are always lower even considering the (low) error affecting the computed values. The observed differences are small, as can be expected on the basis of the simplicity of the adopted reaction model that involves only short range guest-host interactions and intentionally excludes the diffusive approach of the reactants from the reactive dynamics. Further simulations with an increased intermolecular coupling lead to a larger difference between $k_{(\text{silicalite})}$ and $k_{(\text{ZK4})}$; at the same time the general trend (i.e., the relative order of the rates in the three environment) does not change after modifying the internal potential parameters so as to loosen the *A*-*B* ''bond.'' This seems to prove that the qualitative features observed are not entirely determined by the internal force field of the reactive complex and the influence of the environment, albeit small, plays an important role in driving the transfer reaction. It has been shown that, as long as the dynamics of the *activated* complex is concerned, the energetic and mechanical behavior of the reactive system is not solvent dependent. Therefore the observed rate differences should arise mainly from the different ''preparation'' of the activation process, which is driven by the environment. The stronger interactions with the more confining silicalite framework together with the hindering of the transfer when the complex is located in the ZK4 windows seem to be the main structural effects determining the observed behavior. The short range of the intermolecular forces results in the participation of a small number of oxygen atoms to the reactive process. This was shown by calculating the work done on the triatomic complex by each zeolite oxygen in the interval following the barrier crossing, which by symmetry (time-reversibility of the MD trajectories) is equivalent to the barrier climbing step. Both positive and negative work is done on the reagents and there is a large compensation between atoms depositing energy in the reactive complex and atoms removing energy from it. The total work done by the two zeolites is similar and negative, as the energy flux after the barrier crossing is directed from the triatomic complex to the environment. However a different efficiency is shown by the few ''active'' oxygen atoms of silicalite and ZK4, the latter doing a smaller amount of work than the corresponding ones of silicalite; this point may play an important role in determining the rate differences observed on longer time scales.

ACKNOWLEDGMENTS

We are grateful to MURST, University of Sassari and Consiglio Nazionale delle Ricerche for financial support.

[1] M. P. Allen and D. J. Tildesley, *Computer Simulation of Liquids* (Clarendon, Oxford, 1987).
[2] P. Demontis and G. B. Suffritti, Chem. Rev. **97**, 2845 (1997).
[3] P. Demontis, G. B. Suffritti, and A. Tilocca, J. Chem. Phys. **105**, 5586 (1996).
[4] F. Delogu, P. Demontis, G. B. Suffritti, and A. Tilocca, Nuovo Cimento D **19**, 1665 (1997).
[5] F. Delogu, P. Demontis, G. B. Suffritti, and A. Tilocca, J. Chem. Phys. **109**, 2865 (1998).
[6] P. Demontis, G. B. Suffritti and A. Tilocca, J. Phys. Chem. B (in press).
[7] M. P. Allen and P. Schofield, Mol. Phys. **39**, 207 (1980).
[8] M. P. Allen, Mol. Phys. **40**, 1073 (1980).
[9] D. Chandler, J. Stat. Phys. **42**, 49 (1986).
[10] G. Ciccotti, in *Computer Simulation in Material Science*, edited by M. Meyer and V. Pontikis, NATO ASI Series E, Vol.205 (Kluwer Academic, Dordrecht, 1991).
[11] H. van Koningsveld, H. van Bekkum, and J. C. Jansen, Acta Crystallogr., Sect. B: Struct. Sci. **43**, 127 (1987).
[12] J. J. Pluth and J. V. Smith, J. Am. Chem. Soc. **102**, 4704 (1980).
[13] R. M. Whitnell and K. R. Wilson, in *Reviews in Computational Chemistry*, edited by K. B. Lipkowitz and D.B. Boyd, Vol. IV (VCH, New York, 1993).
[14] J. G. Harris and F. H. Stillinger, Chem. Phys. **149**, 163 (1990).
[15] J. P. Bergsma, J. R. Reimers, K. R. Wilson, and J. T. Hynes, J. Chem. Phys. **85**, 5625 (1986).
[16] I. Benjamin, B. J. Gertner, N. J. Tang, and K. R. Wilson, J. Am. Chem. Soc. **112**, 524 (1990).
[17] J. Chandrasekhar and W. L. Jorgensen, J. Am. Chem. Soc. **107**, 2975 (1985).
[18] J. P. Bergsma, B. J. Gertner, K. R. Wilson, and J. T. Hynes, J. Chem. Phys. **86**, 1356 (1987).
[19] B. J. Gertner, R. M. Whitnell, K. R. Wilson, and J. T. Hynes, J. Am. Chem. Soc. **113**, 74 (1991).
[20] J. D. Evanseck, J. F. Blake, and W. L. Jorgensen, J. Am. Chem. Soc. **109**, 2349 (1987).
[21] M. Ben-Nun and R. D. Levine, J. Phys. Chem. **96**, 1523 (1992).
[22] *Proceedings of the 12th International Zeolite Conference*, Baltimore, 1998 edited by M. M. J. Treacy, B. K. Marcus, M. E. Bisher, and J. B. Higgins (Material Research Society, Warrendale, 1999).
[23] I. Benjamin, L. L. Lee, Y. S. Li, A. Liu, and K. R. Wilson, Chem. Phys. **152**, 1 (1991).

[24] S. Jost, S. Fritzsche and R. Haberlandt, Chem. Phys. Lett. **279**, 385 (1997).
[25] S. Bandyopadhyay and S. Yashonath, J. Phys. Chem. **99**, 4286 (1995).
[26] P. Demontis, G. B. Suffritti, S. Quartieri, A. Gamba, and E. S. Fois, J. Chem. Soc., Faraday Trans. **87**, 1657 (1991).
[27] D. Chandler, *Introduction to Modern Statistical Mechanics* (Oxford University, New York, 1987).
[28] D. Chandler, J. Chem. Phys. **68**, 2959 (1978).
[29] D. Brown and J. H. R. Clarke, J. Chem. Phys. **92**, 3062 (1990).
[30] J. A. Montgomery, D. Chandler, and B. J. Berne, J. Chem. Phys. **70**, 4056 (1979).
[31] R. Chitra and S. Yashonath, J. Phys. Chem. B **101**, 5437 (1997).
[32] M. Hayoun, M. Meyer, and P. Turq, J. Phys. Chem. **98**, 6626 (1994).
[33] R. L. June, A. T. Bell, and D. N. Theodorou, J. Phys. Chem. **95**, 8866 (1991).
[34] T. Mosell, G. Schrimpf, C. Hahn, and J. Brickmann, J. Phys. Chem. **100**, 4571 (1996).
[35] T. Mosell, G. Schrimpf, and J. Brickmann, J. Phys. Chem. **100**, 4582 (1996).
[36] T. R. Forester and W. Smith, J. Chem. Soc., Faraday Trans. **93**, 3249 (1997).
[37] B. M. Ladanyi and J. T. Hynes, J. Am. Chem. Soc. **108**, 585 (1979).
[38] R. L. June, A. T. Bell, and D. N. Theodorou, J. Phys. Chem. **96**, 1051 (1992).
[39] J. Kärger, P. Demontis, G. B. Suffritti, and A. Tilocca, J. Chem. Phys. **110**, 1163 (1999).
[40] G. B. Woods and J. S. Rowlinson, J. Chem. Soc., Faraday Trans. 2 **85**, 765 (1989).
[41] I. Ohmine, J. Chem. Phys. **85**, 3342 (1986).
[42] R. A. Kuharski, D. Chandler, J. A. Montgomery, Jr., F. Rabii, and S. J. Singer, J. Phys. Chem. **92**, 3261 (1988).
[43] J. E. Straub, M. Borkovec, and B. J. Berne, J. Chem. Phys. **89**, 4833 (1988).
[44] M. A. Wilson and D. Chandler, Chem. Phys. **149**, 11 (1990).